IMAGE PROCESSING IN MICROWAVE HOLOGRAPHY FOR DIELECTRIC OBJECTS

F. Arndt, P. Ballerscheff, H. Volkmann, and R. Wedekin

Microwave Department, University of Bremen,
Kufsteiner Str. NW1, D-2800 Bremen, W. Germany
EWD, Funkschneise 5-13, D-2800 Bremen, W. Germany

Resumé

Ce papier presente une technique utilisable pour le traitement d'image en appuyant sur la méthode de l'holographie en micro-ondes pour les objets plans diélectriques de diffusion. La simulation numérique des hologrammes avec la transformation discrète de FRESNEL-KIRCHHOFF complétée par un terme de diffraction pour inclure les objets diélectriques offre l'avantage de pouvoir étudier systématiquement les conditions importants de traitement d'image. La reconstruction numérique d'image au moyen de la transformation de FRESNEL permet une technique rapide avec l'usage de l'algorithme FFT à deux dimensions. La simulation des hologrammes est verifiée par des mesurages appropriés. Les résultats de la reconstruction d'image démontrent que l'identification sûre des objets rectanguliers est possible, même pour une modique permittivité relative. Afin de mettre la limite de résolution en évidence par un exemple, on a choisi un objet diélectrique plus compliqué en forme des caractères "RW" en verre (permittivité relative 6).

1. Introduction

Microwave holography is a versatile technique widely used for imaging remote, inaccessible or concealed objects[1-7], as well as for diagnosing errors in large surface profiles, e.g. reflectors[8]. A reliable identification of two- or three-dimensional metallic objects is possible by using single frequency or, for higher axial resolution requirements, multifrequency techniques. Moreover, a suitable numerical second-order technique has been developed for hologram simulation[4,7], by which the required parameters may be systematically investigated in order to improve the accuracy of the imaging method. For dielectric objects, so far, the problem has hitherto not yet been suitably attacked.

The objective of this paper is to present an efficient hologram simulation theory, and a computer-aided image reconstruction technique for plane dielectric objects. For an appropriate theoretical description of the scattering properties, the complex reflection coefficient of the structure is derived using the relations of the geometrical optics, which allow to include all relevant parameters, such as permittivity, thickness, angle of incidence, size and shape. For the computer simulation, FRESNEL- KIRCHHOFF's diffraction integral is utilized in its discrete form together with a suitably extended object function. The image reconstruction step is carried out digitally, where the FRESNEL-approximation enables the use of standard signal processing methods like the Fast-Fourier-Transform (FFT) technique.

Summary

An efficient imaging technique for scattering dielectric plane objects is presented which is based on microwave holographic methods. FRESNEL-KIRCHHOFF's diffraction integral in its discrete form with a suitably extended object function provides an appropriate numerical hologram simulation by which the relevant imaging parameters may be systematically investigated. The image reconstruction is carried out digitally, where the FRESNEL approximation enables the use of standard FFT techniques. Comparison between simulated and measured holograms verifies the numerical simulation technique. The results of the numerical image reconstruction show that a reliable identification of the dielectric objects is possible. The efficiency of the signal processing method is demonstrated at the image reconstruction of a more complicated dielectric object (glass, with a permittivity of 6) shaped in form of the letters "RW" by utilizing a computer simulated hologram.

2. Theory

The computer simulation of the diffracted wave at the point P_{il} in the hologram plane (Fig. 1) is calculated by FRESNEL-KIRCHHOFF's diffraction integral in its discrete form[7].

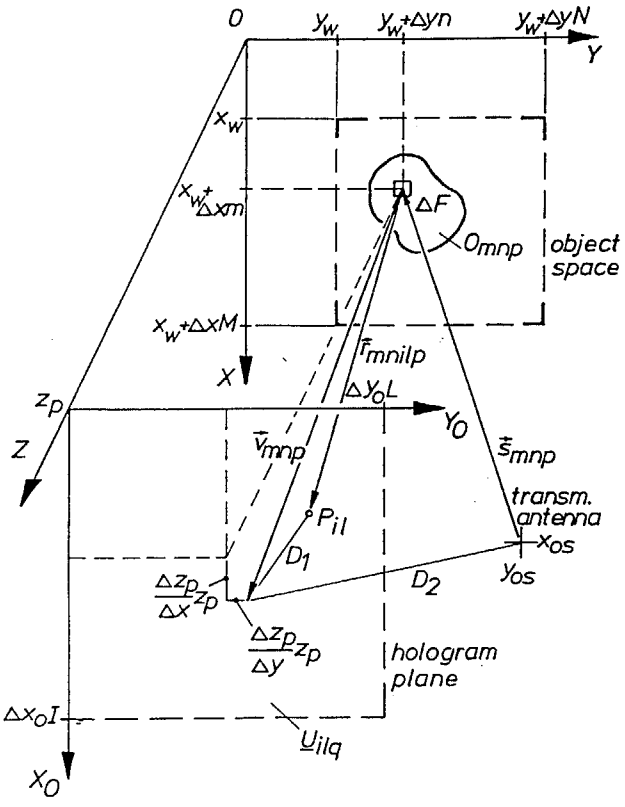

Fig. 1 Object and hologram plane

The complex hologram function $\underline{U}_{ilq}(z)$ is taken for I•L points with the sample distance Δx_0, Δy_0

$$\underline{U}_{ilq}(z) = j\frac{1}{2\lambda_q}\sum_{p=1}^{P-1}\Delta x\Delta y\Delta z_p \sum_{m=0}^{M-1}\sum_{n=0}^{N-1} O_{mnp}C_s \frac{e^{-jk_q s_{mnp}}}{s_{mnp}} \underline{R}_{mnpq} \qquad (1)$$

$$\frac{e^{-jk_q r_{mnilp}}}{r_{mnilp}} \left\{\cos(\vec{v}_{mnp},\vec{r}_{mnilp}) - \cos(\vec{v}_{mnp},\vec{s}_{mnp})\right\}$$

with $\lambda_q = \frac{c}{f_q}$ = wavelength

$k_q = \frac{2\pi}{\lambda_q}$

$O_{mnp}C_s$ = field distribution of the diffracting surfaces

$$s_{mnp} = \left\{(x_{os} - x_w - \Delta x_p m)^2 + (y_{os} - y_w - \Delta y_p n)^2 + z_p^2\right\}^{1/2}$$

$$r_{mnilp} = \left\{(\Delta x_o i - x_w - \Delta x_p m)^2 + (\Delta y_o l - y_w - \Delta y_p n)^2 + z_p^2\right\}^{1/2}$$

$\vec{v}_{mnp} = \vec{n}_{mnp} v_{mnp}$ $\quad \vec{n}_{mnp}$ = direction of the area element ΔF

$$v_{mnp} = z_p\left\{1 + \left(\frac{\Delta z_p}{\Delta x}\right)^2 + \left(\frac{\Delta z_p}{\Delta y}\right)^2\right\}^{1/2}$$

$$\cos(\vec{v}_{mnp},\vec{r}_{mnilp}) = \frac{r_{mnilp}^2 + v_{mnp}^2 - D_1^2}{2 r_{mnilp} v_{mnp}}$$

$$\cos(\vec{v}_{mnp},\vec{s}_{mnp}) = \frac{s_{mnp}^2 + v_{mnp}^2 - D_2^2}{2 s_{mnp} v_{mnp}}$$

$$D_1^2 = (\Delta x_o i - (x_w + \Delta xm) - \frac{\Delta z_p}{\Delta x} z_p)^2 + (\Delta y_o l - (y_w + \Delta yn) - \frac{\Delta z_p}{\Delta y} z_p)^2$$

$$D_2^2 = (x_{os} - (x_w + \Delta xm) - \frac{\Delta z_p}{\Delta x} z_p)^2 + (y_{os} - (y_w + \Delta yn) - \frac{\Delta z_p}{\Delta y} z_p)^2$$

The general form of equation (1) includes the application of the multifrequency holography technique and is written for threedimensional objects, which can be subdivided in P planes with the dimensions $\Delta x \cdot M$, $\Delta y \cdot N$. The subscript q denotes the discrete frequency used. For the numerical examples (dielectric plates) with P=1 calculated in this paper, however, already the monofrequent holographic imaging technique provides sufficient resolution of the object shape.

The scattering characteristics of the plane dielectric object are included by the complex reflection coefficient $\underline{R}_{mnq}$ which is based on the uniform geometrical theory of diffraction (UTD)[9]. The subscript q denotes the frequency, and mn is the number of the related rectangular object segment of size $\Delta x \cdot \Delta y$

$$\underline{R}_{mnq} = \frac{r_1 \cdot (1 - r_2 \cdot r_3)}{1 - r_1^2 \cdot r_2 \cdot r_3} \qquad (2)$$

The coefficients in (2) are given by

$$r_1 = \frac{\cos\varphi - \sqrt{\epsilon_{rmn} - \sin^2\varphi}}{\cos\varphi + \sqrt{\epsilon_{rmn} - \sin^2\varphi}} \qquad (3)$$

$$r_2 = \exp\left\{\frac{-j4\pi\sqrt{\epsilon_{rmn}} \cdot d}{\lambda_q \cdot \sqrt{1 - (\sin^2\varphi)/\epsilon_{rmn}}}\right\} \qquad (4)$$

$$r_3 = \exp\left\{\frac{j4\pi d \cdot \sin^2\varphi / \sqrt{\epsilon_{rmn}}}{\lambda_q \cdot \sqrt{1 - (\sin^2\varphi)/\epsilon_{rmn}}}\right\} \qquad (5)$$

φ is the angle of the reflected wave, and d is the thickness of the dielectric slab section mn (Fig. 2) with the relative permittivity $\epsilon_{rmn} = \epsilon_{2mn}/\epsilon_1$.

$$E^r_{tot} = E^r_1 + E^r_2 + \cdots \qquad E^t_{tot} = E^t_1 + E^t_2 + \cdots$$

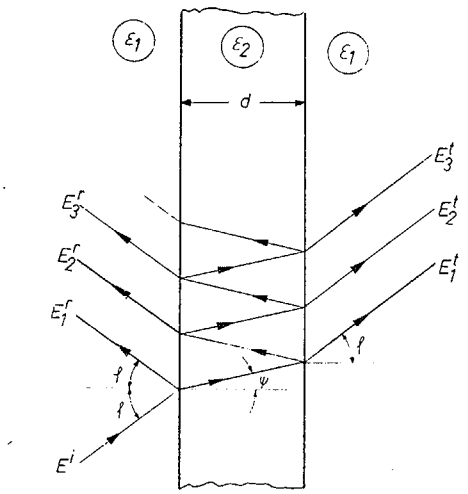

Fig. 2 Plane wave incidence on a dielectric layer of thickness d in free space

The numerical image reconstruction is carried out with the inverse discrete FRESNEL - Transform[7]

$$\underline{O}_{mnq}(z) = -j\frac{\Delta x_o \Delta y_o}{\lambda_q z \underline{R}_{mnq}} s_{mn} e^{jk_q s_{mn}} e^{jk_q z} j\frac{k_q}{2z}\left\{(x_w + \Delta xm)^2 + (y_w + \Delta yn)^2\right\} \qquad (6)$$

$$\sum_{i=0}^{I-1}\sum_{l=0}^{L-1} \underline{U}_{ilq} e^{j\frac{\pi}{\lambda_q z}\left\{(\Delta x_o i)^2 + (\Delta y_o l)^2\right\}} e^{-j\frac{2\pi}{\lambda_q z}\left\{(x_w + \Delta xm)\Delta x_o i + (y_w + \Delta yn)\Delta y_o l\right\}}$$

by which the image function $\underline{O}_{mnq}$ is calculated for the mn object segments and for a discrete frequency denoted by q. For the multifrequency holography technique, a weighted sum[7] of all image functions at Q frequency samples is utilized. If I and L in (6) are chosen appropriately, standard two-dimensional FFT-subroutines may be used.

3. Results

A glass plate (ϵ_r= 6.5) of size 48cm × 48cm with a thickness of 8mm (Fig. 3 a) was chosen for a first example to demonstrate the

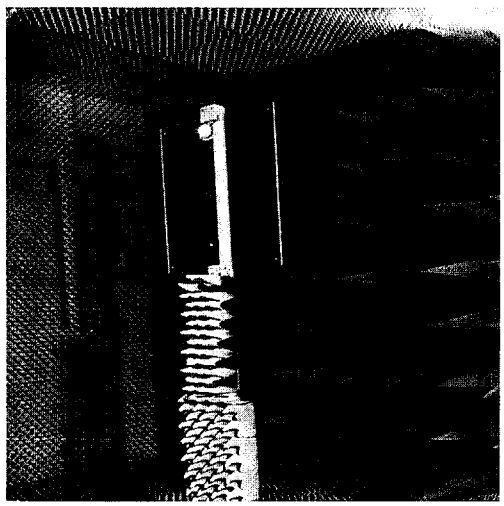

Fig. 3a Glass plate (ϵ_r=6.5) of size 48cm × 48cm, thickness 8mm.

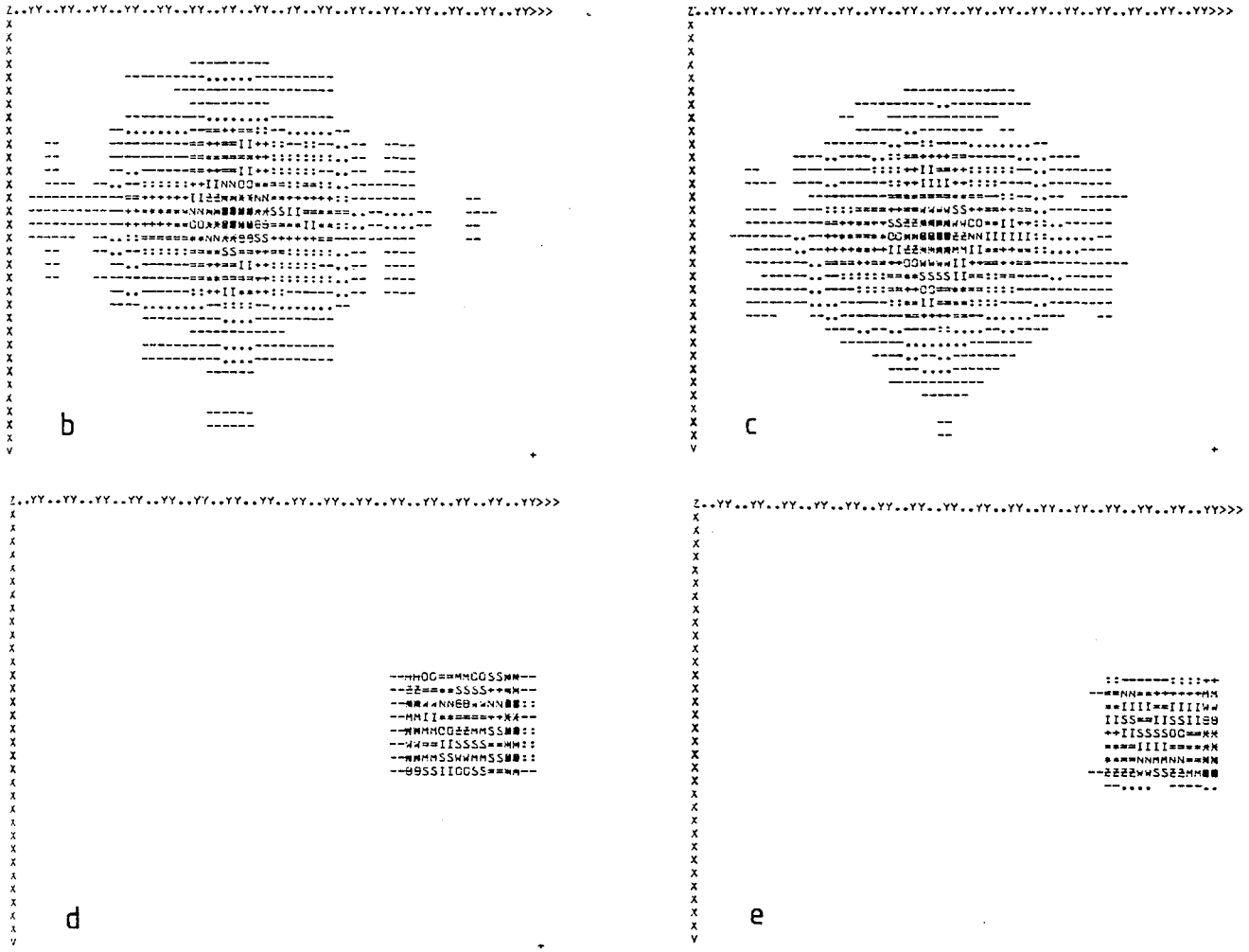

Fig. 3 b-e Glass plate (ϵ_r=6.5). b)Computer simulated hologram using equations (1)-(5). c)Measured hologram. d)Image reconstruction from the simulated hologram, and e)image reconstruction from the measured hologram using equ. (6). Position of the transmitting antenna (cf. Fig 1): x_{0s}=1m, y_{0s}=2.5m; sample point distances in the hologram and object plane: $\Delta x=\Delta y$=6mm; number of sample points: M=N=32. Wavelength λ = 3cm. Size of the hologram and object plane: 1.92m × 1.92m. Distance between object and hologram plane z_p = 4m.

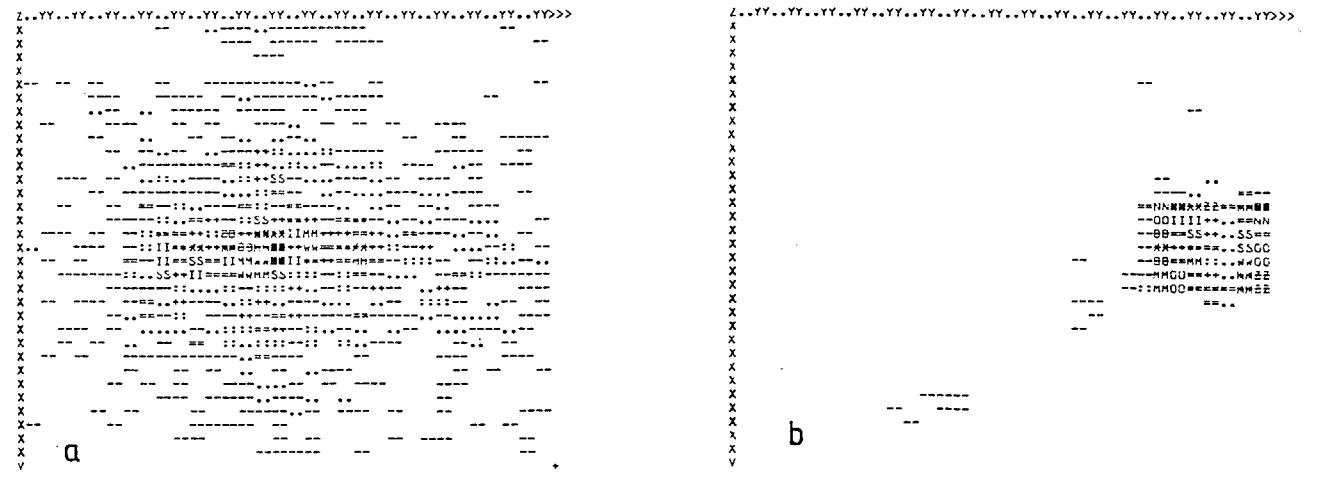

Fig. 4 Plexiglass plate (ϵ_r=2.5). a) Measured hologram. b) Image reconstruction from the measured hologram using equation (6). Data of the measuring equipment and for the reconstruction cf. Fig. 3.

efficiency of the computer simulation of holograms and the numerical reconstruction of plane dielectric objects by comparison with the corresponding measured results, c.f. Figs. 3b - 3e. The dynamic range of the measured and reconstructed values of about 40dB is displayed by a logarithmic gray scale simulated by corresponding letters of the printer. For the image reconstruction, all points below -24dB of the maximum value are suppressed. Good agreement between computer simulated and measured results may be stated. Moreover, the dielectric plate is clearly imaged at the correct position in its original

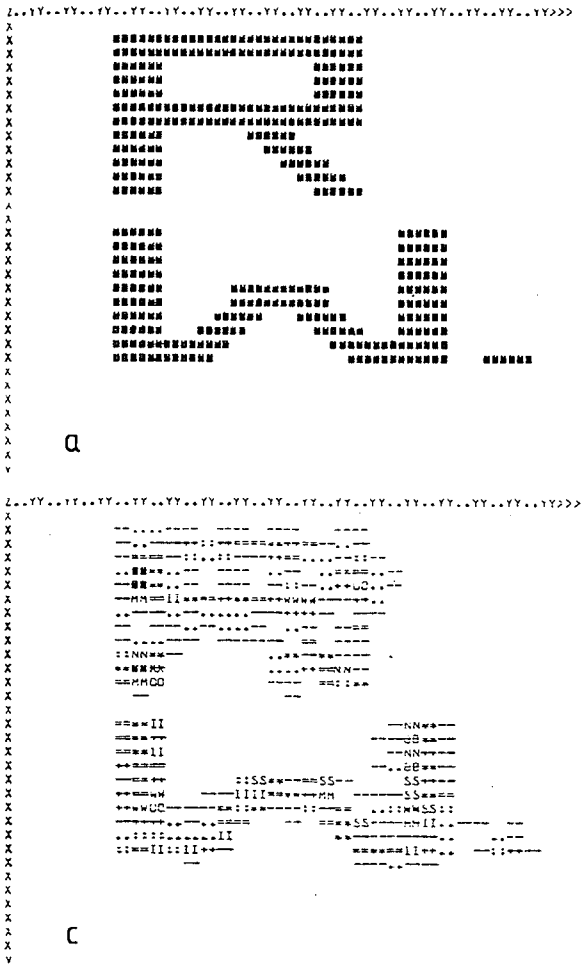

Fig. 5 Plane dielectric object (glass, ϵ_r=6, thickness 8mm) shaped in the form of the letters "RW". The small width (12cm, 4λ) of the bars of the letter "R" chosen violates the sampling theorem for spatial spectra. The width (18cm, 6λ) of the bars of the letter "W", however, meets the sampling theorem. a) Computer simulation of the objects under consideration. b) Computer simulated hologram according to (1)-(5). c) Image reconstruction according to (6). Other simulation and reconstruction data cf. Fig. 3 b-e. Wavelength λ = 3cm.

A plexiglass plate (ϵ_r=2.5) of size 48cm × 48cm with a thickness of 20mm chosen for the second example demonstrates (Fig. 4) that a clear image reconstruction (Fig. 4b) from the measured hologram (Fig. 4a) may be obtained using the discrete FRESNEL-Transform(6), also for dielectric plates with low permittivity values.

The efficiency and the limitations of the hologram simulation and image reconstruction method investigated are demonstrated in Figs. 5 for the more complicated plane dielectric object shaped in form of the letters "RW" . The dielectric material chosen is glass (ϵ_r=6) with a thickness of 8mm. The width (12cm, 4λ) of the bars of the letter "R" chosen violates the sampling theorem for spatial spectra[4] by which the minimum size of the object dimensions x_{obj}, y_{obj} for the chosen data is limited to

$$x_{obj} \geq \frac{2\eta\lambda z}{\Delta x_0 I} = 12.5\text{cm}, \quad y_{obj} \geq \frac{2\eta\lambda z}{\Delta y_0 L} = 12.5\text{cm} \quad . \quad (7)$$

η = 1 is the first minimum of the spatial sinc-function considered, the distance z and the dimensions $\Delta x_0 I$, $\Delta y_0 L$ of the hologram plane are the same as in Figs. 3b-e: z = z_p=4m, 1.92m × 1.92m. Consequently the image resolution of the letter "R" in Fig. 5c is not of sufficient quality. The clear identification of the letter "W", however, demonstrates the accuracy of the numerical hologram simulation and image reconstruction method presented in this paper.

References

1. G. Tricoles, and N.H. Farhat, "Microwave holography: Applications and techniques." Proc. IEEE, Vol. 65, No. 1, pp. 108-121, Jan. 1977
2. A.P. Andersom,"Developments in microwave imaging."Proc. 9th European Microwave Conf., Brighton, pp. 64-73, Sept. 1979
3. R. Karg, "Multifrequency holography." Arch. El. Übertrag., AEÜ-31, pp. 150-156, 1977
4. F. Arndt, and P. Ballerscheff, "Calculations and measurements of holograms and numerical reconstruction of images in the microwave region." Proc. 7ieme Coll. Traitement du Signal et ses Applications, Nice, pp. 111/1-111/6, May 1979
5. F.J. Paolini, and M.J.Duffy, "Digital image reconstruction of microwave holograms". IEEE Trans. Ant. Propagat., Vol. AP-31, pp. 389-393, March 1983
6. N. Osumi, and K. Ueno, "Microwave holographic imaging of underground objects." IEEE Trans. Ant. Propagat., Vol. AP-33, pp. 152-158, Feb. 1985
7. P. Ballerscheff, and F. Arndt, "Numerical processing of multifrequency microwave holography." Proc. 10ieme Coll. Traitement du Signal et ses Applications, Nice, pp. 729-734, May 1985
8. Y. Rahmat-Samii, "Microwave holography of large reflector antennas - Simulation algorithms." IEEE Trans. Ant. Propagat., Vol. AP-33, pp. 1194-1203, Nov. 1985
9. W.D. Burnside, and K.W. Burgener, "High frequency scattering by a thin lossless dielectric slab." IEEE Trans. Ant. Propagat., Vol. AP-31, pp. 104-110, Jan. 1983